

See discussions, stats, and author profiles for this publication at:
<https://www.researchgate.net/publication/228512812>

A theoretical study on the molecular and electronic structure of heteroaromatic bowl-shaped molecules

ARTICLE *in* CHEMICAL PHYSICS LETTERS · JANUARY 2001

Impact Factor: 1.9 · DOI: 10.1016/S0009-2614(00)01345-2

CITATIONS

15

READS

16

3 AUTHORS, INCLUDING:



Minh Tho Nguyen

University of Leuven

748 PUBLICATIONS 10,363 CITATIONS

SEE PROFILE



L. G. Vanquickenborne

University of Leuven

174 PUBLICATIONS 3,355 CITATIONS

SEE PROFILE

A theoretical study on the molecular and electronic structure of heteroaromatic bowl-shaped molecules

David Delaere, Minh Tho Nguyen ^{*}, Luc G. Vanquickenborne

Department of Chemistry, University of Leuven, Celestijnenlaan 200F, B-3001 Leuven, Belgium

Received 16 June 2000; in final form 9 November 2000

Abstract

Geometries, inversion barriers, local aromaticities and vertical excitation energies of four heteroaromatic coronenes including (triphenylenetri)-pyrrole, (-)-furan, (-)-phosphole and (-)-thiophene were computed using MO and DFT methods, and compared with those of coronene and corannulene. The barriers to bowl-to-bowl inversion amount to 297, 183 and 8 kJ/mol for O-, N- and S-forms, respectively, thus the recently synthesized thiophene derivative is a floppy bowl-shaped species. The P-derivative exhibits an almost planar form. NICS values point out that the bowl-shaped molecules have similar local aromaticity in the six-membered rings but differ in those of the five membered rings. The excitation energies were evaluated using the DFT-RPA method. © 2001 Elsevier Science B.V. All rights reserved.

1. Introduction

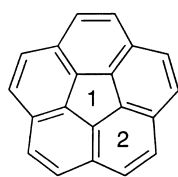
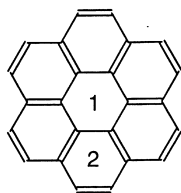
There has been considerable interest in the class of non-alternant hydrocarbons such as corannulene (**I**, C₂₀H₁₀), owing to their unique structures and properties [1]. The molecule (**I**) was first synthesized in 1966 [2,3] and showed to have a bowl-shaped structure with a five-fold axis [4]. Because three corannulene skeletons could formally lead to the construction of a soccer-ball type structure, the connection of these ‘bucky-bowl’ molecules with C₆₀ fullerenes chemistry appears obvious [5]. Despite the substantial curvature present in corannulene, it is highly fluxional and the bowl-to-bowl inversion is rapid [6], the resulting non-rigidity of its bowl structure is in contrast to that of

fullerenes. The first synthesis of a bowl-shaped heteroaromatic compound was recently reported by Tetsuo Otsubo et al. [7]. The triphenylenetri-thiophene **2b** is build up from a central hexagonal ring with a periphery of alternating benzenoid aromatic and thiophene rings. They concluded that the electronic structure of **2b** is similar to that of the highly symmetrical coronene (**II**). Unlike planar coronene, **2b** is a bowl-shaped molecular structure, which has clearly been proven by X-ray crystallographic analysis. The crystal structure belongs to the hexagonal crystal system which is rather unusual for organic molecules [7]. According to these authors those non-planar heteroaromatics could form a basis for novel organic conductors [8].

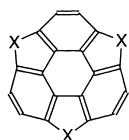
The synthesis of (triphenylenetri)-thiophene (**2b**) and the attempts to synthesize other heteroaromatics [8] motivated us to investigate the molecular and electronic structure of **2b** and of yet unknown analogues such as (triphenylenetri)-

^{*} Corresponding author. Fax: +32-16-327992.

E-mail address: minh.nguyen@chem.kuleuven.ac.be (M. Tho Nguyen).

**I****II**

pyrrole **1a**, (-)-furan **1b** and (-)-phosphole **2a**. Our primary interest lies in finding out whether some of these heteroaromatic structures are rigid. Inversion barriers were thus computed to figure out if bowl-to-bowl inversion is possible. Another question of interest concern an important property being their aromaticity for which a qualitative evaluation has been made. Furthermore, to assist further experimental studies, we assigned the peaks in the absorption spectra of the well-known corannulene (**I**), coronene (**II**) as well as **2b** by computing the corresponding low-lying singlet excitation energies and thereby a prediction was made of the absorption spectra for the other heteroaromatics.



1a: X=NH triphenylenetri-pyrrole
1b: =O -furan
2a: =PH -phosphole
2b: =S -thiophene

2. Computational details

Geometries were first optimized using the Hartree–Fock method in conjunction with the 3-21G* basis set. Analytic harmonic vibrational frequency calculations were done at this level to characterize the nature of stationary points on the potential energy surface and to estimate their zero-point vibrational energies (ZPEs). Subsequently, B3LYP density functional theory computations [9] employing a split valence plus polarisation SV(P) basis set were used to improve the structural data. Chemical shifts at the centers of the pentagons and hexagons, termed as nucleus-independent chemical shifts NICS [10], were evaluated making use of the

GIAO-HF/3-21G* method. Ionization energies (IEs) were obtained from negative HOMO-energies (Koopmans' theorem) using both Hartree–Fock and DFT/B3LYP methods. The low-lying excited states were treated within the adiabatic approximation of time dependent density functional theory (DFT-RPA) [11]. The three-parameter Lee–Yang–Parr (B3LYP) functional proposed by Becke was employed. Additionally the HF based SCI method was used to allow comparison with a more traditional molecular orbital method of comparable computational cost. The calculations of excitation energies were performed in the SV(P) basis. The GAUSSIAN 98 program [12] was used for HF optimizations, analytical frequency analysis and calculating NICS values. On the other hand the Turbomole program [13] was employed for B3LYP optimizations and to compute low-lying transition energies. Note that throughout this Letter, energies are given in kJ/mol, bond lengths in Å and bond angles in degrees.

3. Results and discussion

3.1. Geometries and strain

As illustrated in Fig. 1, the calculated minimum energy conformations of the derivatives **1a**, **1b** and **2b** are bowl-shaped with C_{3v} symmetry. Due to the presence of puckered and strongly pyramidal phosphorus atoms, triphenylenetriphosphole **2a** is characterized by two conformers (C_s and C_{3v}), which are calculated to have similar energy (Fig. 2). As we would like to compare **2a** with the other bowl-shaped heteroaromatics, only the C_{3v} conformer will further be considered. Selected structural data for the C_{3v} bowl-shaped molecules are given in Table 1 including the distance C–X and the angle CXC as well as the bowl depth **h** (Fig. 1), which allows a quantitative determination of the bowl-shaped geometry. The bowl depth is measured by the distance between the plane defined by the six central (core) carbon atoms and the plane defined by the six peripheral (rim) carbon atoms (Fig. 1). The C–X distances are about 0.4–0.5 Å shorter and the CXC angles about 15° larger in the first-row heteroaromatic bowl-shaped

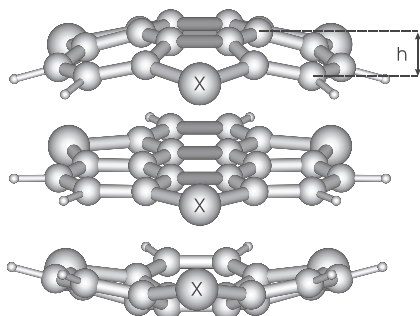


Fig. 1. Bowl-to-bowl inversion of heteroaromatic bowl-shaped molecules (X = NH, O, S).

molecules **1a** and **1b** as compared with the second-row analogues **2a** and **2b**. These structural differences result in more curved or more deeply bowl-shaped first-row heteroaromatic molecules featuring larger *h* values, compared to the second-row ones. Thus, the bowl-shaped heteroaromatics become deeper in the following order: **2a** < **2b** < **1a** < **1b** with (triphenylenetri)-phosphole **2a** being the shallowest and (triphenylenetri)-furan **1b** the most bowl-shaped heteroaromatic molecule. Note that the bowl-depth of corannulene (**I**) amounts 0.86 Å (Fig. 3) and is situated between those of **2b** and **1a**.

The bowl-shaped heteroaromatic structures are obtained from planar coronene (**II**) by replacing the three peripheric benzenoid aromatic rings by heterocyclic five-membered rings in keeping the C_{3v} symmetry. As a consequence, the bowl-shaped heteroaromatics distinguish oneself by their heterocyclic five-membered rings of which the geometry and energy changes will further be discussed.

The strain energy introduced into the five-membered rings by fusing them within a coronene type structure is recorded in Table 2. Correlating $\Delta E_{\text{fused-D}_{3h}/\text{free}}$ towards the bowl depth *h* (Table 1), it is clear that the larger the strain introduced in the planar D_{3h} -structure, the more bowl-shaped becomes the resulting heteroaromatic. The energy difference ($\Delta E_{\text{fused-C}_{3v}/\text{free}}$) between the free five-membered rings and the corresponding ones having the geometry as in the C_{3v} bowl-shaped minima, shows the molecule is curving till the strain in the five-membered ring is reduced to about 50 kJ/mol. As for exception, in the puckered phosphole molecule the strain is reduced towards 42 kJ/mol. The changes induced by the bowl-to-bowl inversion on the geometry and energy of the heterocyclic five membered rings are presented in Table 2. For all planar heterocyclic five-membered rings (pyrrole, furan and thiophene), there is an increase in the C–X bond length and CXC bond angle going from the bowl-shaped (C_{3v}) towards the planar (D_{3h}) structure. The changes turn out to be larger within both first-row heteroaromatics **1a** and **1b**. They are more bowl-shaped and therefore the structural differences with respect to the corresponding planar D_{3h} -structures are more pronounced. As a consequence the energy differences between the five-membered rings in both are much larger for pyrrole and furan (115 and 158 kJ/mol, respectively) as compared with thiophene (20 kJ/mol).

(Triphenylenetri)-phosphole **2a** represents a particular case in that a flattening of the bowl-shaped structure involves in the mean time a flattening of the phosphorus atoms, which induces

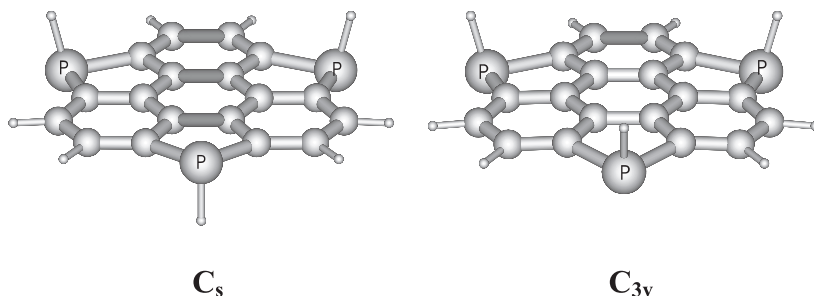
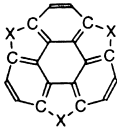


Fig. 2. Geometries of two forms of (triphenylenetri)-phosphole **2a**.

Table 1

Calculated structural characteristics of heteroaromatic bowl-shaped molecules (C_{3v}) at the B3LYP/SV(P) level^a

	X	C–X	CXC	<i>h</i>
		(Å)	(°)	(Å)
1a	NH	1.416 (1.374)	109.0 (109.9)	1.33
1b	O	1.398 (1.356)	106.0 (107.4)	1.50
2a	PH	1.892 (1.818)	91.2 (90.3)	0.13
2b	S	1.809 (1.731)	92.4 (91.7)	0.64

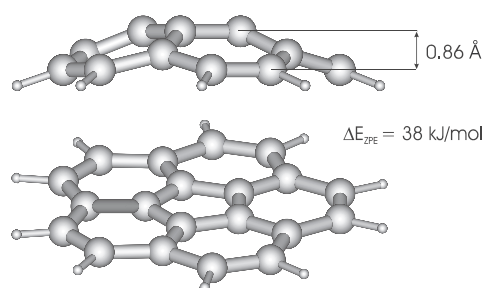
^a Between brackets are given the values for the corresponding free five-membered heterocycles.

Fig. 3. Bowl-to-bowl inversion of corannulene (I) at B3LYP/SV(P) level.

large changes in C–X bond length and CXC bond angle compared to the corresponding structural changes in pyrrole, furan and thiophene (Table 2). More precisely, the bond length is decreasing by 0.104 Å and the bond angle is increasing by 8.5°. Therefore, even though (triphenylenetri)-phosphole **2a** is the shallowest heteroaromatic, the energy difference between the phosphole moiety in both bowl-shaped (C_{3v}) and planar (D_{3h}) structures amounts to 73 kJ/mol.

3.2. Inversion barriers

Fig. 1 schematically illustrates the calculated bowl-to-bowl inversion of the considered heteroaromatic bowl-shaped molecules. Table 3 reports the calculated total energies (E_{Tot}) and ZPE of both C_{3v} -bowl and D_{3h} -planar structures and their energy differences (ΔE_{Tot} and $\Delta E_{\text{ZPE}} = \Delta E_{\text{Tot}} + \Delta ZPE$), which represent the inversion barriers. Frequency analysis point out that the C_{3v} -bowl conformations are all equilibrium structures and the D_{3h} -planar conformations of **1a**, **1b** and **2b** are all transition state structures characterized by one imaginary vibrational frequency of a_2'' symmetry. As for an exception, the D_{3h} -planar form of **2a** is characterized by three imaginary frequencies corresponding the phosphorus atom inversions with vibrational motions of a_2'' and e'' symmetry. Therefore, it can be concluded that planar **2a** is not involved in a bowl-to-bowl inversion. As described above, the first-row heteroaromatics (**1a** and **1b**) are more bowl-shaped and the structural differences towards the planar D_{3h} -structures more pronounced, compared to the

Table 2

Energy differences (ring strain) between corresponding free and fused heterocyclic five-membered rings. Differences in geometrical parameters and energies (ring strain) between five-membered rings in planar (D_{3h}) and bowl-shaped (C_{3v}) heteroaromatics. All calculations performed at the B3LYP/SV(P) level

		$\Delta E_{\text{fused-}D_{3h}/\text{free}}$	$\Delta E_{\text{fused-}C_{3v}/\text{free}}$	$\Delta C-X_{D_{3h}/C_{3v}}$	$\Delta CXC_{D_{3h}/C_{3v}}$	$\Delta E_{D_{3h}/C_{3v}}$
1a	Pyrrole	167	52	0.047	1.4	115
1b	Furan	210	52	0.072	1.2	158
2a	Phosphole	38	42	0.104	8.5	73
2b	Thiophene	71	51	0.014	0.5	20

Table 3

Calculated bowl-to-bowl inversion barriers for heteroaromatic bowl-shaped molecules at the B3LYP/SV(P) level

Structure	C _{3v} -bowl		D _{3h} -planar		Inversion barrier	
	<i>E</i> _{Tot} (hartree)	ZPE (kJ/mol)	<i>E</i> _{Tot} (hartree)	ZPE (kJ/mol)	ΔE_{Tot} (kJ/mol)	ΔE_{ZPE} (kJ/mol)
1a	−854.38773	638	−854.31847	183	182	183
1b	−913.89542	532	−913.78179	531	298	297
2a	−1714.01092	591	−1713.87496	580	357	347
2b	−1882.67738	515	−1882.67461	516	7	8

second-row (triphenylenetri)-thiophene **2b**. Therefore, larger inversion barriers are expected and indeed calculated for **1a** and **1b** as compared with **2b** (Table 3). The inversion barrier for the shallow (triphenylenetri)-thiophene **2b** amounts to only 8 kJ/mol, thus predicting a quasi-spontaneous bowl-to-bowl inversion. The inversion barriers for (triphenylenetri)-pyrrole **1a** and (triphenylenetri)-furan **1b** amount to 183 and 297 kJ/mol, respectively. For the sake of information note that the energy difference between D_{3h}-planar and C_{3v}-bowl (triphenylenetri)-phosphole **2a** is equal to 347 kJ/mol which represents the inversion of three pyramidal phosphorus atoms. This value cannot be compared with those obtained for the other compounds. The corresponding experimental value for the inversion barrier in corannulene (Fig. 3) was reported to be 43 kJ/mol ([6] cf. Introduction). The B3LYP computations in this work pointed to a value of 38 kJ/mol for this quantity, which is comparable to that obtained in an earlier theoretical study [14]. Thus it appears that the thiophene derivative **2b**, which presents the smallest bowl-to-bowl inversion barrier is a floppy molecule, whereas the first-row heteroaromatics **1a** and **1b** are computed to be quite rigid.

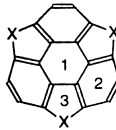
3.3. Local aromaticities as measured by NICS values

Reflecting the ring current flows in polycyclic molecules, the computed NICS values can help to identify areas of higher local aromaticity or anti-aromaticity [10,15]. As mentioned in the introduction and shown in Table 4, three different types of rings can be distinguished in the considered heteroaromatics. The central six-membered ring formed by the core carbon atoms is labeled as **1**

and the NICS-1 value (Table 4) indicates that it is non-aromatic. That is also true for the central six-membered ring in coronene (**II**) which is characterized by a NICS-1 value of +0.8 ppm. On the other hand the NICS-1 value for the central five-membered ring in corannulene (**I**) is calculated at +6.0 ppm which points to a weakly anti-aromatic ring. The NICS-2 values support the view that the peripheric six-membered rings are aromatic. For the heteroaromatics, all NICS-2 values are consistently higher than −9.9 ppm, which is the NICS value calculated for benzene at the same level of theory. That is also the case for the peripheric six-membered rings in coronene (**II**), where a value of −10 ppm is computed. However in corannulene (**I**) the NICS-2 value amounts to −7.9 ppm which is lower than the NICS value of −9.9 ppm for benzene. Finally, the heterocyclic five-membered rings labeled as **3**, drop seriously in terms of aromaticity as seen in the NICS-3 values. The latter can in fact be compared to their free analogues whose NICS values are given between brackets. According to

Table 4

Calculated NICS values (ppm) at the centers of the pentagons and hexagons using the GIAO-HF/3-21G* method^a

	NICS 1	NICS 2	NICS 3
			
1a	−0.2	−13.9	−9.5 (−14.8)
1b	−1.2	−14.3	−6.1 (−12.5)
2a	−1.9	−11.2	1.0 (−4.8)
2b	−1.1	−12.1	−6.4 (−13.4)

^a Between brackets are given the NICS values for the corresponding free five-membered heterocycles. The NICS value for benzene amounts −9.9 ppm.

the NICS-3 values, while the pyrrole rings (**1a**) remain aromatic, the furan (**1b**) and thiophene (**2b**) rings become weakly aromatic and phosphole rings (**2a**) are non-aromatic. The decrease in aromaticity in the heterocyclic five membered rings is associated with an increase in C–X bond length (Table 1). Finally, it can be concluded that the bowl-shaped molecules have similar local aromaticity in the six-membered rings but differ from each other in the aromaticity of the five-membered rings.

3.4. Low-lying electronic excitations

According to the Koopmans' theorem the negative of the HOMO energy corresponds to the vertical ionization energy (IE) or vertical excitation energy of an electron into the continuum. Therefore, it is trivial to mention that the DFT-RPA method is only reliable for excitation energies

smaller than the molecular IE or $\Delta E_{\text{ex}} < |\varepsilon_{\text{HOMO}}|$. According to the Franck–Condon principle, the highest intensity (λ_{max}) in an absorption spectrum also corresponds to a vertical excitation since the electronic excitation is fast with respect to nuclear relaxation. For the considered molecules, the lowest allowed excitations correspond to singlet $\pi \rightarrow \pi^*$ transitions. These low-lying singlet states were computed and assigned to the observed absorption peaks (λ_{max}) in the experimental absorption spectrum of the synthesized compounds (**I**, **II** and **2b**). Table 5 presents the estimated first IE for all molecules considered in this work. In Table 6 are collected the first allowed singlet $\pi \rightarrow \pi^*$ transition energies, which correspond to the lowest HOMO \rightarrow LUMO excitations and are a measure for the energy gap. In Tables 7–12 are given the low-lying $\pi \rightarrow \pi^*$ transitions for corannulene, coronene and the heteroaromatic bowl-shaped molecules, respectively.

The results presented in Table 5 reveal the IEs are computed 1.5–2.0 eV lower using the DFT/B3LYP method as compared with the HF-method. The photoelectron spectrum of corannulene (**I**) shows a first ionization peak at 8.1 eV [16]. The corresponding IE is calculated to be 8.17 and 6.12 eV using the HF and B3LYP methods, respectively. For coronene (**II**) the experimental first IE amounts 7.29 eV [17] and is computed 7.15 and 5.61 eV by HF and B3LYP, respectively. In general, the orbital energies obtained from HF-wavefunctions are larger than the experimental ionization energies [18,19]. On the other hand, the

Table 5
First IEs (eV) given by $-\varepsilon_{\text{HOMO}}$ (Koopmans' theorem)

Structure	HF/SV(P)	B3LYP/SV(P)	Expt. (eV)
I	8.17	6.12	8.10 ^a
II	7.15	5.61	7.29 ^b
1a	6.71	4.82	
1b	7.89	5.86	
2a	7.87	6.00	
2b	7.72	5.75	

^a Ref. [16].

^b Ref. [17].

Table 6
First allowed singlet $\pi \rightarrow \pi^*$ transitions^a

Structure	State	DFT-RPA (eV)	SCI (eV)	Expt. (eV)
I	1^1A_1	4.02 (0.10E – 1)	5.89 (0.44E – 1)	4.35 ^b
II	1^1E_{1u}	4.12 (0.67)	5.81 (2.40)	4.09 ^c , 4.07 ^d
1a	1^1A_1	3.34 (0.12E – 1)	4.43 (0.38E – 1)	
1b	1^1A_1	3.54 (0.97E – 2)	4.69 (0.28E – 1)	
2a	1^1A_1	3.80 (0.13E – 5)	4.93 (0.30E – 4)	
2b	1^1A_1	3.51 (0.75E – 3)	4.70 (0.11E – 2)	3.37 ^e

^a Oscillator strengths are given within parentheses.

^b Ref. [2,3].

^c Ref. [20].

^d Ref. [17].

^e Ref. [7].

Table 7
Singlet $\pi \rightarrow \pi^*$ transitions in corannulene **I**^a

State	DFT-RPA (eV)	SCI (eV)	Expt. ^b (eV)
1^1A_2	3.50 (0.00)	4.65 (0.00)	
1^1E_2	3.53 (0.00)	4.62 (0.00)	
2^1E_2	3.81 (0.00)	4.80 (0.00)	
1^1A_1	4.02 (0.10E – 1)	5.89 (0.44E – 1)	4.35
1^1E_1	4.34 (0.25)	6.07 (0.82)	4.88
2^1E_1	5.27 (0.22)	6.69 (0.98)	
3^1E_2	5.43 (0.00)	7.20 (0.00)	
3^1E_1	5.60 (0.12)	7.15 (0.44)	
4^1E_1	5.74 (0.78E – 1)	8.13 (0.23)	
4^1E_2	5.78 (0.00)	7.94 (0.00)	
5^1E_1	5.81 (0.50E – 1)	8.39 (0.95)	
5^1E_2	5.83 (0.00)	8.15 (0.00)	
2^1A_2	6.00 (0.00)	8.13 (0.00)	
2^1A_1	6.10 (0.12E – 1)	7.82 (0.65E – 1)	

^a Oscillator strengths are given within parentheses.

^b Refs. [2,3]. $\epsilon_{\text{HOMO}} = -6.12$ eV.

DFT method tends to strongly underestimate the IE due to the insufficient cancellation of the self-interaction error in the Hartree-term [19]. In any cases these values allow a qualitative comparison to be made. The HF-method predicts the heteroaromatic bowl-shaped molecules **1b**, **2a** and **2b** to have similar vertical IEs around 7.8 eV, which lies in between the value for corannulene (**I**, 8.17 eV) and coronene (**II**, 7.15 eV). (Triphenyle-

notri)-pyrrole **1a** has the smallest vertical IE (6.71 eV).

Results in Table 6 indicate that for the heterocyclic bowl-shaped structures (**1a**, **1b**, **2a**, **2b**), the singlet state corresponding to the lowest allowed $\pi \rightarrow \pi^*$ transition has A_1 symmetry. The same is found for corannulene (**I**), but for coronene (**II**) the lowest allowed $\pi \rightarrow \pi^*$ state has E_{1u} symmetry. Note that the $X^1A_1 \rightarrow ^1E_{1u}$ transition has a much stronger oscillator strength than the $X^1A_1 \rightarrow ^1A_1$ transitions. The lowest first allowed $\pi \rightarrow \pi^*$ transition energy is computed for (triphenylenetri)-pyrrole (**1a**) to be 3.34 eV with a corresponding oscillator strength of $0.12E - 1$. The first allowed singlet $\pi \rightarrow \pi^*$ transition is similar for (triphenylenetri)-furan (**1b**) and (-)-thiophene (**2b**) and the transition energy is computed around 3.5 eV, with oscillator strengths of $0.97E - 2$ and $0.75E - 3$, respectively. (Triphenylenetri)-phosphole (**2a**) has the highest first allowed $\pi \rightarrow \pi^*$ transition energy (3.80 eV) among the heterocyclic bowl-shaped molecules but with the weakest oscillator strength ($0.13E - 5$). Nevertheless, the first allowed singlet $\pi \rightarrow \pi^*$ transition for corannulene and coronene is still higher and occur at 4.0 eV. Computed vertical excitation energies for corannulene (**I**) are given in Table 7 and a comparison is made with values derived from the experimental absorption spectrum. Barth and Lawtom [2,3]

Table 8
Singlet $\pi \rightarrow \pi^*$ transitions in coronene **II**^a

State	DFT-RPA (eV)	SCI (eV)	Expt. (eV)
1^1B_{1u}	3.20 (0.00)	4.16 (0.00)	3.03 ^b , 2.90 ^c (α -band, 1^1B_{2u})
1^1B_{2u}	3.42 (0.00)	4.13 (0.00)	3.65 ^b , 3.63 ^c (p-band)
1^1E_{1u}	4.12 (0.67)	5.81 (2.40)	4.09 ^b , 4.07 ^c (β -band)
1^1E_{2g}	4.30 (0.00)	5.49 (0.00)	
1^1A_{2g}	4.32 (0.00)	5.43 (0.00)	
1^1A_{1g}	4.40 (0.00)	6.13 (0.00)	
2^1A_{2g}	4.54 (0.00)	6.64 (0.00)	
2^1E_{2g}	4.63 (0.00)	5.72 (0.00)	
3^1E_{2g}	4.93 (0.00)	7.19 (0.00)	
2^1A_{1g}	5.03 (0.00)	7.15 (0.00)	
4^1E_{2g}	5.19 (0.00)	7.27 (0.00)	
5^1E_{2g}	5.38 (0.00)	7.87 (0.00)	
2^1B_{1u}	5.45 (0.00)	7.47 (0.00)	

^a Oscillator strengths are given within parentheses.

^b Ref. [20].

^c Ref. [17]. $\epsilon_{\text{HOMO}} = -5.61$ eV.

Table 9

Singlet $\pi \rightarrow \pi^*$ transitions in (triphenylenetri)-pyrrole **1a**^a

State	DFT-RPA (eV)	SCI (eV)
1^1A_2	3.27 (0.00)	4.31 (0.00)
1^1A_1 (α -band)	3.34 (0.12E – 1)	4.43 (0.38E – 1)
1^1E p-band	3.60 (0.16)	4.98 (0.54)
2^1E	4.56 (0.16E – 2)	5.89 (0.79E – 2)
2^1A_2	4.81 (0.00)	6.22 (0.00)
2^1A_1	4.84 (0.12E – 3)	6.72 (0.82E – 2)
3^1E	4.90 (0.13E – 2)	6.29 (0.20)

^aOscillator strengths are given within parentheses.
 $\epsilon_{\text{HOMO}} = -4.82$ eV.

Table 10

Singlet $\pi \rightarrow \pi^*$ transitions in (triphenylenetri)-furan **1b**^a

State	DFT-RPA (eV)	SCI (eV)
1^1A_1 (α -band)	3.54 (0.97E – 2)	4.69 (0.28E – 1)
1^1A_2	3.55 (0.00)	4.48 (0.00)
1^1E (p-band)	3.92 (0.18)	5.24 (0.48)
2^1E	4.41 (0.10E – 3)	5.77 (0.72E – 1)
3^1E	4.85 (0.35E – 1)	6.40 (0.28)
2^1A_2	4.99 (0.00)	6.45 (0.00)
2^1A_1	5.00 (0.40E – 2)	7.03 (0.28E – 1)
4^1E (β -band)	5.13 (0.20)	6.99 (0.37)
3^1A_2	5.32 (0.00)	7.52 (0.00)
5^1E	5.36 (0.86E – 1)	7.64 (0.35)
3^1A_1	5.45 (0.44E – 1)	7.72 (0.29)
6^1E	5.51 (0.64E – 2)	7.90 (0.45E – 1)
4^1A_2	5.65 (0.00)	8.24 (0.00)

^aOscillator strengths are given within parentheses.
 $\epsilon_{\text{HOMO}} = -5.86$ eV.

described the UV-spectrum to be remarkable for his simplicity as well as for the very sharp absorption at 4.88 eV. In this work, the experimentally observed absorption peak at 4.35 eV is assigned to the weak 1^1A_1 state computed at 4.02 eV with an oscillator strength of 0.10E – 1. The sharp absorption at 4.88 eV is assigned to the 1^1E_1 state computed at 4.34 eV with an oscillator strength of 0.25. We have also located two higher intense absorption peaks of E_1 symmetry: the 2^1E_1 state at 5.27 eV with an oscillator strength of 0.22 and the 3^1E_1 state at 5.60 eV with an oscillator strength of 0.12.

Table 8 records the vertical excitation energies for coronene (**II**) whose experimental electronic

Table 11

Singlet $\pi \rightarrow \pi^*$ transitions in (triphenylenetri)-phosphole **2a**^a

State	DFT-RPA (eV)	SCI (eV)
1^1A_1 (α -band)	3.80 (0.13E – 5)	4.93 (0.30E – 4)
1^1A_2	3.98 (0.00)	4.71 (0.00)
1^1E	4.02 (0.25E – 2)	5.27 (0.19E – 1)
2^1E (p-band)	4.43 (0.33)	5.90 (0.11)
2^1A_2	4.92 (0.00)	6.31 (0.00)
2^1A_1	4.94 (0.94E – 4)	6.73 (0.16E – 1)
3^1E	4.94 (0.47E – 1)	6.35 (1.83)
4^1E	4.98 (1.00E – 2)	6.98 (0.27E – 1)
5^1E (β -band)	4.98 (0.16)	7.28 (0.67E – 1)
3^1A_2	5.00 (0.00)	7.43 (0.00)
3^1A_1	5.09 (0.28E – 3)	7.54 (0.99E – 4)
6^1E	5.14 (0.83E – 1)	7.43 (0.27)
4^1A_2	5.23 (0.00)	7.63 (0.00)
7^1E	5.26 (0.47E – 1)	7.58 (0.18E – 2)
4^1A_1	5.44 (0.47E – 2)	7.89 (0.53E – 1)
5^1A_1	5.84 (0.77E – 3)	8.01 (0.13E – 1)
5^1A_2	5.84 (0.00)	7.87 (0.00)
8^1E	5.84 (0.83E – 2)	7.95 (0.96E – 1)

^aOscillator strengths are given within parentheses.
 $\epsilon_{\text{HOMO}} = -6.00$ eV.

absorption spectrum shows an α -band around 3.0 eV. There are also two bands centered around 3.6 and 4.1 eV, assigned to p- and β -bands, respectively. Inokuchi et al. [20] ascribed the α -band to an electronic transition from the $1A_{1g}$ ground state to the $1B_{2u}$ state, which is symmetry forbidden. According to our calculations the α -band likely corresponds to a transition to the 1^1B_{1u} state at 3.20 eV; the p-band is assigned to the 1^1B_{2u} state located at 3.42 eV. Both transitions are symmetry forbidden. The β -band computed at 4.12 eV is the most intense feature of the spectrum with an oscillator strength of 0.67.

In Table 12 are presented the vertical excitation energies for (triphenylenetri)-thiophene (**2b**), a molecule for which the synthesis, molecular structure and spectroscopic properties were recently reported by Otsubo et al. [7]. These authors described the electronic absorption spectrum in CH_2Cl_2 to show a long-wavelength vibrational α -band at 3.37 eV and suggested this excitation, to be responsible for the yellow coloration of the molecule (the transition being symmetry forbidden). Furthermore, they reported two strong bands centered at 3.90 and 5.06 eV, assigned to p-

Table 12

Singlet $\pi \rightarrow \pi^*$ transitions in (triphenylenetri)-thiophene **2b**^a

State	DFT-RPA (eV)	SCI (eV)	Expt. ^b (eV)
1 ¹ A ₁	3.51 (0.75E – 3)	4.70 (0.11E – 2)	3.37 (α -band)
1 ¹ A ₂	3.60 (0.00)	4.60 (0.00)	
1 ¹ E	3.98 (0.24)	5.64 (0.47)	
2 ¹ E	4.48 (0.13E – 2)	5.76 (0.20)	3.90 (p-band)
2 ¹ A ₂	4.84 (0.00)	6.22 (0.00)	
2 ¹ A ₁	4.85 (0.12E – 2)	6.86 (0.41E – 3)	
3 ¹ E	5.02 (0.59E – 1)	6.28 (0.30E – 1)	5.06 (β -band)
3 ¹ A ₂	5.05 (0.00)	6.45 (0.00)	
4 ¹ E	5.08 (0.64E – 1)	6.43 (0.86)	
4 ¹ A ₂	5.19 (0.00)	7.18 (0.00)	
5 ¹ E	5.21 (0.14)	7.23 (0.91E – 1)	
6 ¹ E	5.25 (0.77E – 4)	7.44 (0.20)	
3 ¹ A ₁	5.28 (0.38E – 2)	7.46 (0.37E – 1)	
4 ¹ A ₁	5.41 (0.15E – 3)	7.77 (0.21E – 2)	
7 ¹ E	5.44 (0.20E – 2)	7.57 (0.11)	
8 ¹ E	5.64 (0.16)	7.85 (0.71E – 1)	

^a Oscillator strengths are given within parentheses.^b Ref. [7], $\epsilon_{\text{HOMO}} = -5.75$ eV.

and β -bands, respectively. Finally, Otsubo et al. [7] concluded that the whole absorption spectrum roughly resembles that of coronene, supporting an iso-electronic structure for both compounds. In the present study, it appears that the α -band can better be assigned to the $X^1A_1 \rightarrow 1^1A_1$ transition at 3.51 eV with an oscillator strength of $0.75E - 3$, which corresponds to an allowed state but with a very weak intensity. The strong p-band is referred to the 1^1E state at 3.98 eV with an oscillator strength of 0.24 and the β -band is assigned to the 5^1E state at 5.21 eV with an oscillator strength of 0.14.

Overall the electronic structure of the bowl-shaped heteroaromatic compounds considered in this work (Tables 9–12) feature a great similarity of low-lying excited states: a weak 1^1A_1 state, an intense 1^1E state and a weak 1^1E state that are the three lowest allowed $\pi \rightarrow \pi^*$ transitions. Such similarity allows us to retrieve the band structure observed in the spectrum of (triphenylenetri)-thiophene (**2b**), which is expected to exist in the spectra of the other heteroaromatics. For this, we were looking for states with the same symmetry and intensity as found in **2b**. Our conclusions are that both (triphenylenetri)-furan (**1b**) and (-)-thi-

ophene (**2b**) have corresponding bands at a comparable energy. For its part, (triphenylenetri)-pyrrole (**1a**) has the lowest α - and p-band, due to the DFT-RPA restrictions we were not able to assign the β -band. On the other hand, (triphenylenetri)-phosphole (**2a**) has the highest α - and p-bands but the lowest β -band. The conclusion drawn by Otsubo et al. suggesting **2b** to be iso-electronic with coronene is not fully supported by our calculations.

In summary, in the present theoretical study, we have shown that (triphenylenetri)-thiophene is a floppy bowl-shaped molecule with a low barrier to inversion of only 8 kJ/mol whereas the bowl-shaped first-row heteroaromatics (N- and O-forms) are computed to be rigid. Comparison of the properties of the bowl-shaped molecules suggest they have similar local aromaticity in the six-membered rings but differ from each other in the aromaticity of the five-membered rings. The bowl-shaped heteroaromatic compounds have also similar low-lying excited states, moreover (triphenylenetri)-furan and (-)-thiophene have corresponding α -, p- and β -bands at comparable levels of energy.

Acknowledgements

The authors are indebted to the FWO-Vlaanderen and KULeuven Research Council (GOA-program) for continuing support.

References

- [1] P.W. Rabidau, A. Sygula, *Acc. Chem. Res.* 29 (1996) 235.
- [2] W. Barth, R. Lawtom, *J. Am. Chem. Soc.* 88 (1966) 380.
- [3] W. Barth, R. Lawtom, *J. Am. Chem. Soc.* 93 (1971) 1730.
- [4] J. Hanson, C. Nordman, *Acta Crystallogr. B* 32 (1976) 1147.
- [5] G. Mehta, P.V.V.S. Sarma, *Chem. Commun.* (2000) 19.
- [6] L. Scott, M. Hashemi, M. Bratcher, *J. Am. Chem. Soc.* 114 (1992) 1920.
- [7] T. Otsubo, K. Imamura, K. Takimiya, Y. Aso, *Chem. Commun.* (1999) 1859.
- [8] See *Chemical Engineering News*, issue October 4, 1999, p. 28.
- [9] R.G. Parr, W. Yang, *Density-Functional Theory of Atoms and Molecules*, Oxford University Press, New York, 1989.
- [10] P.v.R. Schleyer, C. Maerker, A. Dransfeld, H. Jiao, N.J.R.v.E.J. Hommes, *J. Am. Chem. Soc.* 118 (1996) 6317.
- [11] R. Bauernschmitt, R. Ahlrichs, *Chem. Phys. Lett.* 256 (1996) 454.
- [12] M.J. Frisch, et al., *GAUSSIAN 98 Revision A.5*, Gaussian, Inc, Pittsburgh PA, 1998.
- [13] R. Ahlrichs, M. Bär, M. Häser, H. Horn, C. Kölmel, *Chem. Phys. Lett.* 162 (1989) 165.
- [14] P.U. Biedermann, S. Pogodin, I. Agranat, *J. Org. Chem.* 64 (1999) 3655.
- [15] M. Bühl, *Chem. Eur. J.* 4 (1998) 734.
- [16] R. Gleiter, J.S. Siegel, K.K. Baldrige, T.J. Seiders, *Tetrahedron Lett.* 41 (2000) 4519.
- [17] W. Schmidt, E. Clar, *Tetrahedron* 33 (1977) 2093.
- [18] A. Szabo, N.S. Ostlund, *Modern Quantum Chemistry: Introduction to Advanced Electronic Structure Theory*, Dover Publications, New York, 1996.
- [19] R. Stowasser, R. Hoffmann, *J. Am. Chem. Soc.* 121 (1999) 3414.
- [20] K. Ohno, T. Kajiwarra, H. Inokuchi, *Bull. Chem. Soc. Jpn.* 45 (1972) 996.